

# Polaron formation in the presence of Rashba spin-orbit coupling: implications for spintronics

Lucian Covaci and Mona Berciu

*Department of Physics and Astronomy, University of British Columbia, Vancouver, BC, Canada, V6T 1Z1*

(Dated: October 31, 2018)

We study the effects of the Rashba spin-orbit coupling on the polaron formation, using a suitable generalization of the Momentum Average approximation. Contrary to previous investigations of this problem, we find that the spin-orbit interaction decreases the effective electron-phonon coupling. It is thus possible to lower the effective mass of the polaron by increasing the spin-orbit coupling. We also show that when the spin-orbit coupling is large as compared to the phonon energy, the polaron retains only one of the spin polarized bands in its coherent spectrum. This has major implications for the propagation of spin-polarized currents in such materials, and thus for spintronic applications.

PACS numbers: 71.38.-k, 71.70.Ej

In the field of spintronics there is a continued effort to develop means of efficiently manipulating the spin of electrons [1]. One widely studied approach is to use spin-orbit coupling (SO) to lift the spin degeneracy, for example the Rashba SO coupling [2] that arises in a confined system if the quantum well lacks inversion symmetry. Experimentally, the Rashba effect has been seen in many systems, *e.g.* semiconductor heterostructures like GaAs and InAs, surface states of metals like Au(111)[3] and surface alloys like Bi/Ag [4] or Pb/Ag [5].

Confined two-dimensional (2D) systems may also couple strongly to optical phonons of the substrate. Tuning of these electron-phonon (el-ph) interactions was shown to be experimentally viable in organic single-crystal transistors [6]. Strong el-ph coupling is interesting because it leads to polaron creation, whereas the coherent quasiparticle is an electron surrounded by a phonon cloud. The polaron dispersion and effective mass can be significantly renormalized from those of the bare band electron [7].

An interesting question is whether the el-ph and the SO coupling can be used in conjunction to tailor differently the properties of the two bands with different spin. The interplay of the Rashba SO and the el-ph interactions has been considered previously for continuous systems with parabolic bands and weak el-ph coupling, using the self-consistent Born approximation [8]. The main conclusion was that SO enhances the effective el-ph coupling due to a topological modification of the Fermi surface, namely an effective reduced dimensionality of the low energy electronic density of states. In this Letter, we investigate this problem using a suitable generalization of the Momentum Average (MA) approximation [9], which allows us to investigate non-parabolic bands (tight-binding models) for any el-ph coupling strength. This is because this method is accurate for any coupling strength, being exact in the asymptotic limits of both very weak and very strong coupling. We demonstrate that the conclusions of Refs. 8 do not apply in the low density limit for a tight-binding dispersion. In fact, the exact opposite holds, namely the effective el-ph coupling is suppressed by SO coupling.

We also calculate spin-dependent spectral functions and show that in a certain regime, the coherent polaron band is dominated by contributions from only one SO electronic band (the “-” band). This has major implications for spin dependent transport through such materials, allowing for the possibility to manipulate the effective mass and the spin polarization of quasiparticles by tuning the el-ph and SO interactions.

We consider a single electron on a two dimensional square lattice with SO coupling, which also interacts with optical phonons of energy  $\Omega$  ( $\hbar = 1$ ) through a local Holstein-type interaction [10]. The Hamiltonian can be written in terms of  $\mathbf{k}$ -space spinors as:

$$\mathcal{H} = \sum_{\mathbf{k}} \begin{pmatrix} c_{\mathbf{k}\uparrow}^\dagger & c_{\mathbf{k}\downarrow}^\dagger \end{pmatrix} \begin{pmatrix} \epsilon_{\mathbf{k}} & \phi_{\mathbf{k}} \\ \phi_{\mathbf{k}}^* & \epsilon_{\mathbf{k}} \end{pmatrix} \begin{pmatrix} c_{\mathbf{k}\uparrow} \\ c_{\mathbf{k}\downarrow} \end{pmatrix} + \Omega \sum_{\mathbf{q}} b_{\mathbf{q}}^\dagger b_{\mathbf{q}} \\ + \frac{g}{\sqrt{N}} \sum_{\mathbf{k}, \mathbf{q}} \begin{pmatrix} c_{\mathbf{k}-\mathbf{q}\uparrow}^\dagger & c_{\mathbf{k}-\mathbf{q}\downarrow}^\dagger \end{pmatrix} \begin{pmatrix} b_{\mathbf{q}}^\dagger + b_{-\mathbf{q}} & 0 \\ 0 & b_{\mathbf{q}}^\dagger + b_{-\mathbf{q}} \end{pmatrix} \begin{pmatrix} c_{\mathbf{k}\uparrow} \\ c_{\mathbf{k}\downarrow} \end{pmatrix}$$

where  $\epsilon_{\mathbf{k}} = -2t[\cos(k_x a) + \cos(k_y a)]$  is the 2D free-electron dispersion for nearest-neighbor hopping and  $\phi_{\mathbf{k}} = 2V_s[i \sin(k_x a) + \sin(k_y a)]$  describes the Rashba SO coupling. Different dispersions and/or SO couplings can be studied similarly. As usual,  $c_{\mathbf{k},\sigma}^\dagger$  is the creation operator for an electron with momentum  $\mathbf{k}$  and spin  $\sigma$ , while  $b_{\mathbf{q}}^\dagger$  creates a phonon of momentum  $\mathbf{q}$ . Both electron spin channels interact with the phonons through the local lattice displacement, with an el-ph coupling constant  $g$ . The lattice has a total of  $N$  sites and periodic boundary conditions, and in the end we let  $N \rightarrow \infty$ . Momentum sums are over the Brillouin zone (BZ).

The  $2 \times 2$  Green's functions for the non-interacting system (no el-ph coupling) are defined as:

$$\bar{G}_0(\mathbf{k}, \omega) = \langle 0 | \begin{pmatrix} c_{\mathbf{k}\uparrow} \\ c_{\mathbf{k}\downarrow} \end{pmatrix} \hat{G}_0(\omega) \begin{pmatrix} c_{\mathbf{k}\uparrow}^\dagger & c_{\mathbf{k}\downarrow}^\dagger \end{pmatrix} | 0 \rangle \\ = \begin{pmatrix} G_{0+}(\mathbf{k}, \omega) & e^{i\epsilon_{\mathbf{k}}} G_{0-}(\mathbf{k}, \omega) \\ e^{-i\epsilon_{\mathbf{k}}} G_{0-}(\mathbf{k}, \omega) & G_{0+}(\mathbf{k}, \omega) \end{pmatrix} \quad (1)$$

where  $\hat{G}_0(\omega) = [\omega - \mathcal{H}_0 + i\eta]^{-1}$  is the resolvent corresponding to  $\mathcal{H}_0 = \mathcal{H}|_{g=0}$ . The symmetric and anti-

symmetric Green's functions are:

$$G_{0\pm}(\mathbf{k}, \omega) = \frac{1}{2} \left( \frac{1}{\omega + i\eta - \epsilon_k + |\phi_{\mathbf{k}}|} \pm \frac{1}{\omega + i\eta - \epsilon_k - |\phi_{\mathbf{k}}|} \right)$$

and the phase factor is  $\xi_{\mathbf{k}} = \phi_{\mathbf{k}}/|\phi_{\mathbf{k}}|$ . To avoid confusion with scalars, all  $2 \times 2$  matrices will be identified by a bar, hence the  $\bar{G}_0(\mathbf{k}, \omega)$  notation.

The full Green's function, defined as usually:

$$\bar{G}(\mathbf{k}, \omega) = \langle 0 | \begin{pmatrix} c_{\mathbf{k}\uparrow} \\ c_{\mathbf{k}\downarrow} \end{pmatrix} \hat{G}(\omega) \begin{pmatrix} c_{\mathbf{k}\uparrow}^\dagger & c_{\mathbf{k}\downarrow}^\dagger \end{pmatrix} | 0 \rangle, \quad (2)$$

can in principle be calculated exactly by applying the equation of motion method. The full Green's function can be related to the non-interacting one by using the Dyson equation,  $\hat{G}(\omega) = \hat{G}_0(\omega) + \hat{G}(\omega)V\hat{G}_0(\omega)$  - here  $V = \mathcal{H} - \mathcal{H}_0$  is the el-ph interaction. As shown previously for the Holstein Hamiltonian [9, 11, 12], the repeated use of the Dyson identity generates a system of equations involving generalized Green's functions with various numbers of phonons. In the presence of SO interactions, the equations of motion are similar, except they are in terms of  $2 \times 2$  Green's functions. As a result, we can implement the MA approximations in the same way, and all conclusions regarding accuracy for all el-ph coupling strengths, sum rules obeyed exactly by the spectral weight, etc. remain true. A somewhat analogous procedure was used to compute the  $2 \times 2$  Green's function describing rippled graphene [13], however there the matrices are related to different sublattices, not to different spin projections.

For all levels of the MA approximation, the Green's function can be written in the standard form:

$$\bar{G}(\mathbf{k}, \omega) = [\bar{G}_0(\mathbf{k}, \omega)^{-1} - \bar{\Sigma}(\mathbf{k}, \omega)]^{-1}, \quad (3)$$

where the self-energy  $\bar{\Sigma}(\mathbf{k}, \omega)$  has different expressions depending on the level of MA approximation used. For the simplest, least accurate MA<sup>(0)</sup> level [9, 11], the self-energy has no  $\mathbf{k}$  dependence and is given by an infinite continued fraction  $\bar{\Sigma}_{MA^{(0)}}(\omega) = g^2 \bar{A}_1(\omega)$ , defined by

$$\bar{A}_n(\omega) = n\bar{g}_0(\omega - n\Omega)[\mathbb{1} - g^2\bar{g}_0(\omega - n\Omega)\bar{A}_{n+1}(\omega)]^{-1}, \quad (4)$$

where

$$\bar{g}_0(\omega) = \frac{1}{N} \sum_{\mathbf{k}} \bar{G}_0(\mathbf{k}, \omega) = \begin{pmatrix} g_{0+}(\omega) & 0 \\ 0 & g_{0+}(\omega) \end{pmatrix} \quad (5)$$

is the momentum average of the noninteracting Green's function over the BZ. Note that because the off-diagonal part is anti-symmetric, its average over the Brillouin zone vanishes, thus  $\bar{g}_0(\omega)$  and all  $\bar{A}_n(\omega)$  matrices are diagonal.

As discussed extensively in Refs. 11 and 12, MA<sup>(0)</sup> is accurate for ground state properties but it fails to properly predict the polaron+one phonon continuum. As a result, it overestimates the polaron bandwidth. This problem is fixed at the MA<sup>(1)</sup> level, where a phonon is allowed

to appear away from the polaron cloud. For the Holstein model (and by extension, in the presence of SO coupling) both these approximations predict  $\mathbf{k}$ -independent self-energies. Here, they are diagonal as well, *i.e.* phonon emission/absorption is not allowed to scatter the electron between the two spin-polarized bands. These, of course, are approximations, although it is worth pointing that all non-crossed diagrams give  $\mathbf{k}$ -independent and diagonal contributions to the self-energy. This is why the self-consistent Born approximation prediction for the self-energy is also  $\mathbf{k}$ -independent and diagonal [8].

In MA, however, the effect of non-crossed diagrams is included for MA<sup>(2)</sup> and higher levels (in variational terms, these allow two or more phonons to appear away from the main polaron cloud and the order of their creation/annihilation now becomes relevant). We therefore report MA<sup>(2)</sup> results here. Following a similar procedure to that described in detail in Ref. [12], the MA<sup>(2)</sup> self-energy is found as:

$$\bar{\Sigma}_{MA^{(2)}}(\mathbf{k}, \omega) = \bar{x}(0), \quad (6)$$

given by the solution of the system of coupled equations for the unknown  $2 \times 2$  matrices  $\bar{x}(i)$ :

$$\sum_j \bar{M}_{i,j}(\mathbf{k}, \omega) \bar{x}(j) = e^{i\mathbf{k}\cdot\mathbf{R}_i} g^2 \bar{G}_0(-i, \tilde{\omega}). \quad (7)$$

The sum is over lattice sites  $i = (i_x, i_y)$  located at  $\mathbf{R}_i = i_x a \hat{x} + i_y a \hat{y}$ . The  $2 \times 2$  matrices  $\bar{M}_{i,j}(\mathbf{k}, \omega)$  are:

$$\bar{M}_{00} = \mathbb{1} - g^2 \bar{g}_0(\tilde{\omega}) \bar{g}_0(\tilde{\omega}) (2\bar{a}_{31}^{-1} - \bar{a}_{21}^{-1}), \quad (8)$$

$$\bar{M}_{i0} = -g^2 \bar{g}_0(\tilde{\omega}) e^{i\mathbf{k}\cdot\mathbf{R}_i} \bar{G}_0(-i, \tilde{\omega}) (2\bar{a}_{31}^{-1} - \bar{a}_{21}^{-1}) \quad (9)$$

for  $i \neq 0$ , and for both  $i, j \neq 0$ :

$$\bar{M}_{ij} = \bar{a}_{21} \delta_{i,j} \mathbb{1} - g^2 e^{i\mathbf{k}\cdot\mathbf{R}_i} \bar{G}_0(j, \tilde{\omega}) \times [(\bar{A}_2 - \bar{A}_1) \delta_{i,-j} + \bar{G}_0(-i-j, \tilde{\omega}) \bar{a}_{21}^{-1}]. \quad (10)$$

Here we defined  $\bar{a}_{ij} = \mathbb{1} - g^2 \bar{g}_0(\tilde{\omega}) (\bar{A}_i - \bar{A}_j)$  where  $\bar{A}_1 \equiv \bar{A}_1(\omega - 2\Omega)$ ,  $\bar{A}_2 \equiv \bar{A}_2(\omega - \Omega)$ ,  $\bar{A}_3 \equiv \bar{A}_3(\omega)$  are continuous fractions defined by Eq. (4), and  $\tilde{\omega} = \omega - 2\Omega - g^2 \bar{A}_1|_{(1,1)}$ ,  $\tilde{\tilde{\omega}} = \omega - g^2 \bar{g}_0(\tilde{\omega})|_{(1,1)} (\bar{a}_{21}^{-1})|_{(1,1)}$  (since the  $\bar{A}$ ,  $\bar{a}$ ,  $\bar{g}_0$  matrices are proportional to  $\mathbb{1}$ , the (2,2) diagonal matrix element can be used just as well in the definitions of  $\tilde{\omega}$ ,  $\tilde{\tilde{\omega}}$ ). Finally, the real space Green's functions appearing in the inhomogeneous terms are given, as usual, by:

$$\bar{G}_0(i, \omega) = \frac{1}{N} \sum_{\mathbf{k}} e^{i\mathbf{k}\cdot\mathbf{R}_i} \bar{G}_0(\mathbf{k}, \omega). \quad (11)$$

It is important to note that for  $i \neq 0$ ,  $\bar{G}_0(i, \omega)$  acquires off-diagonal components, which lead to the off-diagonal contributions in  $\bar{\Sigma}_{MA^{(2)}}(\mathbf{k}, \omega)$ . Because below the free-electron continuum the  $\bar{G}_0(i, \omega)$  decrease exponentially as  $|\mathbf{R}_i|$  increases, the system in Eq. (7) can be truncated at a small  $|i|$ . We truncate at  $|\mathbf{R}_i| \simeq 10a$ , such that the relative error of the spectral function is less than  $10^{-3}$ .

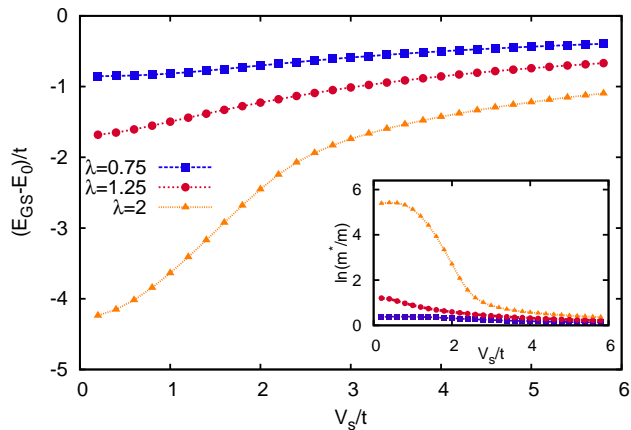


FIG. 1: (color online) The ground state energy as a function of Rashba SO coupling for three values of the el-ph coupling. The inset shows the effective mass on a logarithmic scale as a function of Rashba SO coupling.

Once the self-energy is known, the full Green's function can be calculated and in turn provide accurate estimates for spectral weights, the ground state energy, the effective mass etc. In the non-interacting case ( $g = 0$ ) the ground state consists of four degenerate points in  $\mathbf{k}$ -space,  $(\pm k_{min}, \pm k_{min})$ , where  $k_{min}a = \arctan[V_s/(\sqrt{2}t)]$ , with the ground-state energy  $E_0 = -4t \cos(k_{min}a) - V_s\sqrt{8}|\sin(k_{min}a)|$ . On the other hand, in the absence of SO coupling ( $V_s = 0$ ), as the effective el-ph coupling  $\lambda = g^2/(4t\Omega)$  is turned on, there is a crossover from a light, large-polaron to a very heavy, small-polaron at  $\lambda \sim 1$ . In Fig. 1 we show the ground state energy measured from  $E_0$  for weak, medium and strong effective el-ph couplings, as a function of the Rashba SO coupling. For large SO coupling, the renormalization of the energy and effective mass (shown in the inset) is strongly suppressed, indicating large-polaron behavior even when  $\lambda = 2$ . This contradicts reported results for a parabolic band dispersion [8], which are based on the fact that the density of states at the band edge has a square root singularity, because in a continuum model the locus of momenta defining the ground state is a circle of radius  $k_{min}$ . This is not generically true for a tight binding dispersion, where the Van Hove singularity is shifted from the 4-point degenerate ground state to higher energies. As expected, though, the results for a parabolic dispersion can be recovered by our tight-binding model in the regime where both  $\lambda$  and  $V_s/t$  are very small. Indeed, for  $\lambda = 0.75$ , the effective mass increases slightly with  $V_s$  at small  $V_s$ , before decreasing at larger  $V_s$  values. Such behavior is more apparent as  $\lambda \rightarrow 0$  [14].

Our results can be understood by noting that the free-electron bandwidth increases with increasing  $V_s$ . This results in an effective el-ph coupling, which compares the polaron binding energy to this renormalized bandwidth,

that effectively decreases. As a result, away from the limit where both  $\lambda$  and  $V_s/t$  are very small, an increase in the SO coupling leads to a drop in the effective mass, making it possible to tune the mass of the polaron between heavy and light. Light polarons are thus found for either small  $\lambda$  irrespective of  $V_s/t$ , or at large  $\lambda$  and large enough  $V_s/t$ . As we show next, however, their nature and spin-character may be very different.

The MA<sup>(2)</sup> approximation is quantitatively accurate not only for the ground state, but also for high energy states, as it satisfies exactly the first 8 spectral weight sum rules and with good accuracy all other ones. It is thus possible to have an accurate depiction of the high energy states by calculating the spectral function. Because we expect to have spin polarized bands it is necessary to calculate a spin dependent spectral function:

$$\vec{A}(\mathbf{k}, \omega) = -\frac{1}{\pi} \text{Im}(\text{Tr}[\vec{\sigma} \vec{G}(\mathbf{k}, \omega)]), \quad (12)$$

where  $\vec{\sigma}$  are the Pauli matrices. The direction of  $\vec{A}(\mathbf{k}, \omega)$  gives the direction of the expectation value of the spin, while its magnitude gives the density of states with momentum  $\mathbf{k}$ . We know that in the non-interacting case as we go around the  $\Gamma$ -point, eigenstates have spin perpendicular to their momentum direction and rotating clockwise for one band and anti-clockwise for the other. For the coupled system we observe similar spin eigenstates and thus choose to plot the following quantity:

$$\tilde{A}(\mathbf{k}, \omega) = [\vec{u}_k \times \vec{A}(\mathbf{k}, \omega)] \cdot \vec{u}_z, \quad (13)$$

where  $\vec{u}_k$  and  $\vec{u}_z$  are unit vectors parallel to  $\mathbf{k}$ , respectively  $z$ -axis. The two spin polarized bands will now correspond to opposite signs of  $\tilde{A}(\mathbf{k}, \omega)$ .

Since the polaron bandwidth cannot exceed  $\Omega$ , we expect the character of the polaron band to depend on the relation between  $\Omega$  and the energy difference between the spin-split electron bands. In order to exemplify this we plot  $\tilde{A}(\mathbf{k}, \omega)$  in Fig. 2 for  $\lambda = 1$ ,  $\Omega = 0.8t$  and  $V_s = 0.4t$ . The spectral function is shown along the  $(0, 0)$ - $(\pi, \pi)$  line in order to intersect the ground state at  $(k_{min}, k_{min})$ . In this case  $\Omega/(E_0 - 4t) > 1$  and we see two coherent polaron bands corresponding to the two spin polarizations, with similar quasiparticle weights. We conclude that when  $\Omega$  is larger than the SO splitting, the polaronic quasiparticles are rather similar to the non-interacting electrons, except for the renormalized mass and suppressed quasiparticle weight. Of course, the spectrum above  $E_{GS} + \Omega$  becomes incoherent due to el-ph scattering.

In Fig. 3 we plot  $\tilde{A}(\mathbf{k}, \omega)$  for  $\Omega = 0.2t$ ,  $\lambda = 1.0$  and  $V_s = 0.8t$ . Now  $\Omega/(E_0 - 4t) < 1$  and because the polaron bandwidth cannot exceed  $\Omega$ , it is dominated by the “-” band. There is a large difference between the quasiparticle weights of the two coherent polaron bands (note the different positive and negative scales for the the contour plot), and the effective mass of the dominant “-” band

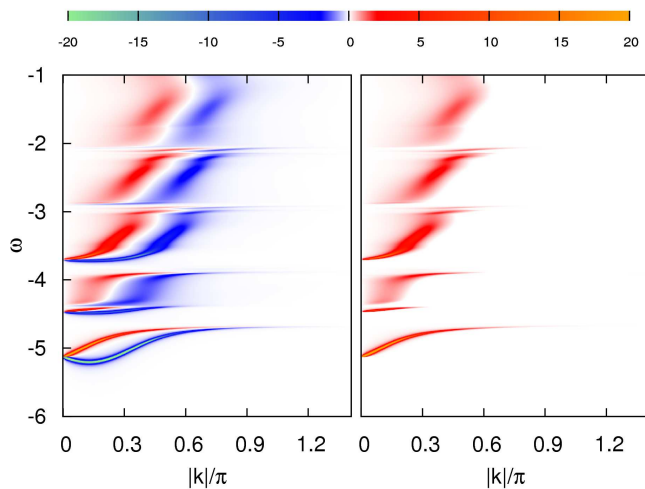


FIG. 2: (color online) Spin dependent spectral function  $\tilde{A}(\mathbf{k}, \omega)$ , for  $\lambda = 1$ ,  $\Omega = 0.8t$  and  $V_s = 0.4t$ . The right panel shows only the “+” band for clarity.

is much smaller than that of the low-weight “+” band. Higher energy states have small weights and are highly incoherent, *i.e.* short lived.

Consider now injection of a current in such a system. Whereas in a regime like that depicted in Fig. 2 we expect the spin to precess between the two coherent polaronic bands, like it does for non-interacting electrons [15, 16], in a regime like in Fig. 3 only the spin-component parallel to the “-” band can be efficiently transmitted through the system, which therefore acts as an intrinsic “spin-polarizer”.

This becomes more and more apparent as one moves further into the asymptotic limit where both the SO and the el-ph couplings are large compared to  $\Omega$ , *i.e.*

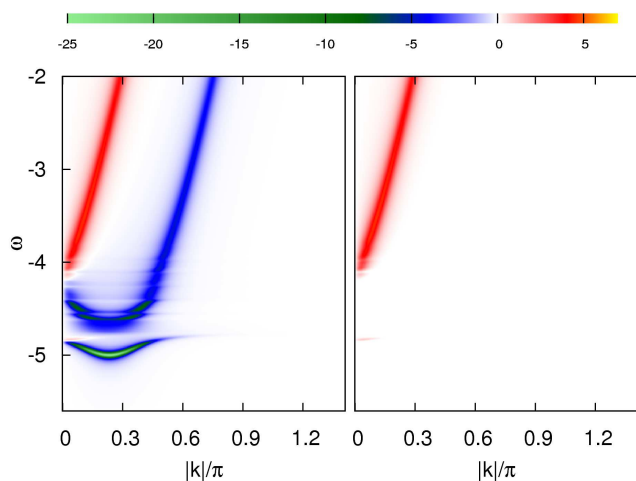


FIG. 3: (color online) Spin dependent spectral function  $\tilde{A}(\mathbf{k}, \omega)$ , for  $\lambda = 1$ ,  $\Omega = 0.2t$  and  $V_s = 0.8t$ . The right-hand side panel shows only the “+” band for clarity.

( $E_0 - 4t$ )  $\gg \Omega$  and  $\lambda \gg 1$ . In this limit the “-” band in the coherent polaron spectrum becomes lighter and has a higher quasiparticle weight, whereas the “+” band essentially vanishes from the coherent spectrum (its quasiparticle weight is extremely low and its effective mass is extremely large). The resulting light polaron is thus very different from the one we find in the small  $\lambda$  regime, which has both bands in the coherent spectrum with roughly equal quasiparticle weights and effective mass.

This demonstrates that an interplay between SO and el-ph couplings allows indeed for different tailoring of the properties of the two spin-polarized bands, whereas one is well described by a long-lived, light quasiparticle while the other becomes highly incoherent. This will naturally lead to very different conductivities for the two spin polarizations, making such a material ideal as a source and/or detector of spin-polarized currents – these are important components needed for many spintronics applications. These conclusions are based on the use of the MA approximation which is known to be highly accurate for all el-ph couplings. Moreover, at the MA<sup>(2)</sup> level we use here, it results in a non-diagonal,  $\mathbf{k}$ -dependent self-energy, therefore our results properly include phonon-mediated scattering between the two electronic bands.

Acknowledgments: This work was supported by CIFAR Nanoelectronics and NSERC. Discussions with Frank Marsiglio are gratefully acknowledged.

- 
- [1] I. Žutić, J. Fabian, and S. Das Sarma, Rev. Mod. Phys. **76**, 323 (2004).
  - [2] E. I. Rashba, Sov. Phys. Solid State **2**, 1224 (1960).
  - [3] S. LaShell, B. A. McDougall, and E. Jensen, Phys. Rev. Lett. **77**, 3419 (1996).
  - [4] C. R. Ast, et al., Phys. Rev. Lett. **98**, 186807 (2007).
  - [5] D. Pacilé, et al., Phys. Rev. B **73**, 245429 (2006).
  - [6] I. H. Hulea et al., Nat. Mater. **5**, 982 (2006).
  - [7] for a review see H. Fehske and S. A. Trugman, in Polarons in Advanced Materials, edited by A. S. Alexandrov (Canopus, Bath/Springer-Verlag, Bath, 2007).
  - [8] E. Cappelluti, C. Grimaldi and F. Marsiglio, Phys. Rev. B **76**, 085334 (2007); *ibid*, Phys. Rev. Lett. **98**, 167002 (2007); F. Marsiglio (private communications).
  - [9] M. Berciu, Phys. Rev. Lett. **97**, 036402 (2006).
  - [10] T. Holstein, Ann. Phys. (N.Y.) **8**, 325 (1959); *ibid* **8**, 343 (1959).
  - [11] G. L. Goodvin, M. Berciu and G. A. Sawatzky, Phys. Rev. B **74**, 245104 (2006).
  - [12] M. Berciu and G. L. Goodvin, Phys. Rev. B **76**, 165109 (2007); M. Berciu, Phys. Rev. Lett. **98**, 209702 (2007).
  - [13] L. Covaci and M. Berciu, Phys. Rev. Lett. **100**, 256405 (2008).
  - [14] L. Covaci and M. Berciu, unpublished.
  - [15] B. Srisongmuang et al., Phys. Rev. B **78**, 155317 (2008).
  - [16] C.A. Perroni et al., J. Phys.: Cond. Matt., **19**, 186227 (2007).